

Image Reconstruction Algorithm of Compressed Sensing based on Neural Dynamics

Zhenhua Gan^{1,2}, Baoping Xiong^{2,3}, Fumin Zou^{*4}, Lyuchao Liao⁴, Min Du²

¹College of Information Science and Engineering, Fujian University of Technology
No.3 Xueyuan Road, University Town, Minhou
Fuzhou City, Fujian Province, China

²College of Electrical Engineering and Automation, Fuzhou University
No.2 Xueyuan Road, University Town, Minhou
Fuzhou City, Fujian Province, China

³Fujian Provincial Key Laboratory of Big Data Mining and Applications
No.3 Xueyuan Road, University Town, Minhou
Fuzhou City, Fujian Province, China

⁴Key Lab of Automotive Electronics and Electric Drive Technology of Fujian Province
No.3 Xueyuan Road, University Town, Minhou
Fuzhou City, Fujian Province, China

ganzh@fjut.edu.cn, xiongbp@qq.com, fmzou@fjut.edu.cn, achao@fjut.edu.cn, dm_dj90@163.com

Received December, 2016; revised March, 2017

ABSTRACT. *To improve the recovery performance of compressed sensing (CS) reconstruction, this paper proposed a CS reconstruction model based on neural dynamics optimization algorithm (NDOA) with l_1 -norm minimization, and applied it to the two-dimensional (2D) image signals to verify the reconstruction effectiveness. Experiments proved the NDOA had performed better in reconstruction than the orthogonal matching pursuit (OMP) and its improved algorithms considering its perfect recovery. When the compressed sampling rate is 0.875 for 64×64 Lena image, the application of NDOA would raise the peak signal to noise ratio (PSNR) by 3.6466dB while decrease the relative error (R_{EOR}) by 2.21% in comparison with OMP and SWOMP. It showed that the effectiveness of CS reconstruction of NDOA was evident. At the same time, the adoption of NDOA could realize real-time processing by parallel computing, which would effectively solve real-time problems such as image processing in the realm of high dimensional sparse signals.*

Keywords: Reconstruction algorithm, Neural dynamics, Compressed sensing, Sparse signal, Image processing.

1. **Introduction.** Compressed sensing (CS) theory provides a powerful support for accurate recovery of sparse signals. It could be implemented in far below the Nyquist-sampling frequency to achieve the perfect reconstruction of original signal, and it has already been widely used in biological sensing, radar detection, data compression, pattern recognition and image processing [1].

Nevertheless, there are some limitations in the application of CS to the processing of two-dimensional (2D) image signals. The [2,3] have introduced the column priority method which reduces the 2D image signals into one-dimensional (1D) signals, and then

directly applies the CS theory to recovering them. However, this process leads to a disastrously increasing in the dimension of the signal and the capacity of measurement matrix. 2D CS model has been proposed in [4,5], which is used to compress and reconstruct the 2D image direct. This method has obtained better results, but the efficiency of the algorithm still need to be improved [6].

As is well known to all, minimizing the l_0 -norm of CS is a NP-hard problem. It is difficult to use conventional computer to solve this sort of problems even if the question is of medium size. Candès et al. have proved that if the measurement matrix satisfied the constraint isometric property (RIP), the l_0 -norm minimization for optimization problem could be quasi convex relaxation to construct the l_1 -norm minimum as an alternative solution [7].

Currently, the most commonly used optimization algorithms are the projection gradient method, the spectral projection gradient method, the conjugate gradient method, the interior point method, the Newton method and the quasi-Newton method. However, these optimization algorithms have been facing high computational complexity and local optimality problems [8]. Since the energy function is introduced into the neural dynamics optimization algorithm (NDOA), the solution of the optimization problem is transformed into the corresponding globally convergent differential equation, which has the advantages of low computational complexity, global optimal solution, parallel computing, and adaptability for hardware implementation and so on. The NDOA has been widely used in image processing, machine control, signal processing and other engineering fields [9,10]. The NDOA, realized by parallel computation of hardware circuits or software programs, has the potential advantage of computing speed, which would effectively solve problems such as 2D signals of CS in real-time processing [11].

This paper offers a novel CS recovery algorithm based on NDOA, whose results show that the superiority and the validity of the proposed method. The rest of the paper is organized as follows. The related knowledge about 2D CS and NDOA are introduced in Section 2. And then, the experimental results and analyses are given in Section 3. Finally, conclusions and discussion are drawn in Section 4.

2. 2D compressive sensing based on the Optimization of NDOA.

2.1. 2D compressive sensing. Suppose a finite length discrete digital signal $f \in R^N$ which was expressed as $x = \psi^T f$, and x was K -sparse in the orthogonal basis $\psi \in R^{N \times N}$. If a measurement matrix $\phi \in R^{M \times N}$ while $M \ll N$ was designed, the CS observations would be shown as below [12,13].

$$y_{M \times 1} = \phi_{M \times N} f = \phi_{M \times N} \psi_{N \times N} x_{N \times 1} = A_{M \times N} x_{N \times 1} \quad (1)$$

however, the equation (1) was an underdetermined system[14].

Since the signal x was K -sparse and x was only K unknown variables on the unknown location, so the freedom of x was only $K+1$ degrees. The high precision recovery of signal x of K -sparse could be obtained by some nonlinear methods when the number of measurements was no less than $K+1$.

CS theory had pointed out that the signal x was K -sparse with $K \ll N$, and we could obtain the accurate recovery of signal x with a measurement matrix A by minimizing the following type of l_0 -norm [15].

$$\hat{x} = \operatorname{argmin} \|x\|_0 \quad s.t. \quad y = Ax \quad (2)$$

where $\|x\|_0$ denoted as the l_0 -norm.

Solving the l_0 -norm was a combinatorial optimization problem, it was well known as a

NP-hard problem. In order to avoid computational difficulties, it was usually converted the l_0 -norm into an l_1 -norm solution with the optimization constraints as long as the measurement matrix A had satisfied the RIP. An l_1 -norm solution was shown as following [16].

$$\hat{x} = \operatorname{argmin} \|x\|_1 \quad s.t. \quad y = Ax \quad (3)$$

where $\|x\|_1 = \sum |x_i|$ with $i=1,2,\dots,N$, denoted as the l_1 -norm. and the formula (3) was usually converted into a linear programming problem to achieve the optimization [8].

For the image signals recovering, firstly, the 2D signals would be transformed into the 1D array through the vector processing, generally. And then, used the formula (2) or (3) directly to recover the 1D signals with a random measurement matrix. However, when the 2D image signals were converted into the 1D array by columnar straightening, their dimension of the matrix sharply increased, at the same time, the spatial relationship of the image elements would be lost. To solve these problems, the [17,18] extended the CS perception and the compression measurement of each column of image was made, to form an equivalent 2D sparse transform. It was still an appropriate choice to recover each column signals of the image by CS algorithm, for reducing the computational complexity, cutting down memory space and decreasing the scale of the measurement matrix.

Consider an image signals $F \in R^{N \times N}$ that can be expressed as $X = WFW^T$, while X were sparse in the orthogonal basis $W \in R^{N \times N}$. We could design $\Phi \in R^{M \times N}$ as a measurement matrix of each column of the image F . So the observed signals $Y \in R^{M \times N}$ would be shown as

$$Y = \Phi F = \Phi W^T X W = \Theta X W \quad (4)$$

Therefore, under the observation $Y W^T \in R^{M \times N}$, the 2D image signals $F = W^T X W$ would be reconstructed by each column vector $x_j \in R^{N \times 1}$ of the sparse image $X \in R^{N \times N}$ with the observation matrix $\Theta \in R^{M \times N}$. And the formula (4) could be conveyed as

$$\min \|x_j\|_0 \quad s.t. \quad Y W^T = \Theta X. \quad j \in [1, N] \quad (5)$$

When the Φ was a normalized matrix subjected to the Gaussian distribution, the $\Theta = \Phi W^T$ had satisfied RIP with high probability. Under these conditions, in order to obtain the constrained optimization solution easily, the formula (5) of the l_0 -norm was relaxed as following

$$\min \|x_j\|_1 \quad s.t. \quad Y W^T = \Theta X. \quad j \in [1, N] \quad (6)$$

2.2. Constrained optimization model based on NDOA. The NDOA provided a powerful tool for solving the constrained optimization of linear programming (LP) and quadratic programming (QP) problems. We were concerned with LP and QP problems of the form

$$\min \left(\frac{1}{2} x^T A x + a^T x \right) \quad s.t. \quad D x = b, \quad x \geq 0 \quad (7)$$

and their dual form

$$\max (b^T y - \frac{1}{2} x^T A x) \quad s.t. \quad D^T - A x \leq a \quad (8)$$

where A was a $p \times p$ real symmetric semi-definite matrix, D was a $p \times p$ real matrix, $x, a \in R^p$, and $y, b \in R^q$.

Assuming that the I was a unit matrix, $(x_i)^+ = \max\{0, x_i\}$, where $i = 1, \dots, p$. By the

[19], we could get the neural network model and obtain numerical solution for differential equations of the problems (7) and (8) as following.

$$\frac{d}{dt} \begin{pmatrix} x \\ y \end{pmatrix} = - \begin{bmatrix} (I + A)[x - (x + D^T y - Ax - a)^+] + D^T(Dx - b) \\ -D[x - (x + D^T y - Ax - a)^+] + Dx - b \end{bmatrix} \quad (9)$$

And the solution of differential equations (9) was a global optimal solution for the formula (7) and (8).

2.3. Compressed sensing reconstruction model based on NDOA. Considering the $\|x\|_1 = \sum |x_i|$, we could divide the sparse signal X into two parts, namely, the positive elements and the negative elements. So, define $X = p - q$, where $p_i = (x_i)^+ = \max\{0, x_i\}$ and $q_i = (-x_i)^+ = \max\{0, -x_i\}$. And then, the $\|x\|_1$ can be expressed as $\|x\|_1 = \mathbf{1}_N^T p + \mathbf{1}_N^T q$ with $\mathbf{1}_N^T = [1 \cdots 1]_{1 \times N}$. Therefore, by the formula (4) there is

$$YW^T = \Theta X = \Theta(p - q) = [\Theta, -\Theta] \begin{bmatrix} p \\ q \end{bmatrix} \quad (10)$$

We expressed the formula (6) as a standard LP optimization model

$$\begin{cases} \min F(u) = \min(c^T u) \\ s.t. \quad Du = b \\ \quad \quad u \geq 0 \end{cases} \quad (11)$$

where $u = [p, q]^T$, $c = \mathbf{1}_{2N}$, $D = [\Theta, -\Theta]$, and $b = YW^T$.

Their dual form was

$$\begin{cases} \max \quad (b^T v) \\ s.t. \quad D^T v \leq c \end{cases} \quad (12)$$

We could obtain the neural network model of the differential equations (11) and (12) based on the formula (10).

$$\frac{d}{dt} \begin{pmatrix} u \\ v \end{pmatrix} = - \begin{bmatrix} u - (u + D^T v - c)^+ + D^T(Du - b) \\ D(u + D^T v - c)^+ - b \end{bmatrix} \quad (13)$$

The u obtained from the differential equations (13) by classical Runge-Kutta method was the global optimization for formula (11) and (12). Since $u = [p, q]^T$, the optimal sparse solution of formula (5) could be deduced from $X = p - q$.

3. Simulation results and analyses.

3.1. The stability of NDOA. According to formula (13), the stability of the solution by NDOA could be evaluated at first. Now supposed that we were presented a set simulation observations of vector x which was subjected to the random distribution individually. Furthermore, the situations of K-sparse non-zero elements in the vector x were also subjected to the random distribution. When the K-sparse non-zero elements had been denoted as $x_k = [-27.8154, -40.5747, 19.2457, -20.1159, 19.1928, -7.5357, -11.3157, -13.8572, 4.6031, -23.6347]$ at $N=96$, $M=48$ and $K=10$, the stability curves of the NDOA solving procedure as shown in Fig.1.

The Fig.1 illustrates that the procedure of NDOA is globally asymptotically stable. And the different curves in the graph correspond to the absolute value of each element of the random vector x . Moreover, the K non-zero elements converge correctly while the other elements converge to zero.

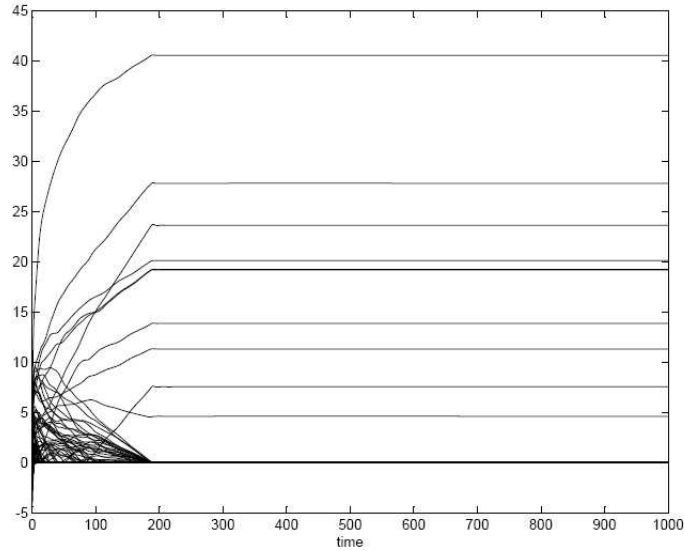


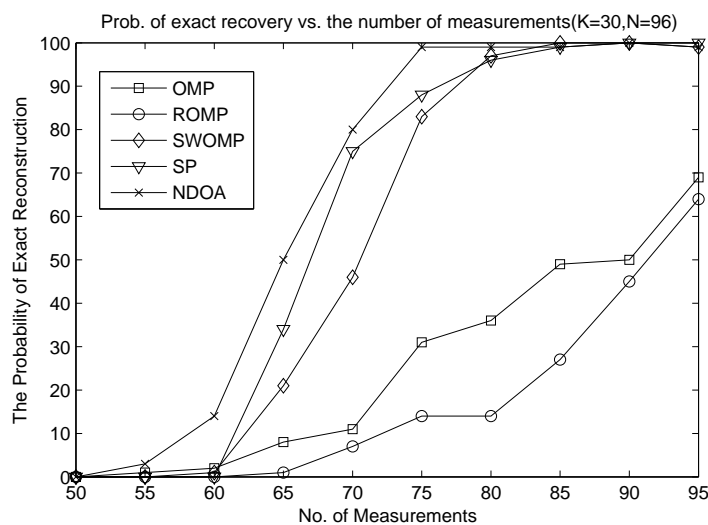
FIGURE 1. Stability of the solution by NDOA

3.2. Simulation experiment of reconstruction algorithm based on NDOA. In order to verify the validity of the presented approach, we had designed the random vector x while $N=96$ and the K -sparse non-zero elements had been subjected to the random distribution, to investigate the performance of CS reconstruction based on NDOA.

At first, we investigated the relations between the reconstructed performance and the number of observations.

For comparison of the reconstruction performance in different algorithms, we designed the random vector x with $K=32$, and respectively performed by OMP, ROMP, SWOMP, SP and NDOA under 100 cycles on the high reconstruction accuracy, i.e., the relative error, $e \leq 1E - 6$. As shown in Fig.2, which is indicated the relations between the reconstruction ratios and the number of observations.

The Fig.2 demonstrates the accurate reconstruction ratio in different algorithms under

FIGURE 2. Accurate recovery probability versus the different observation number M while $N=96$ and $K=32$

the random vector x with $N=96$, $K=32$, while only the number of observations, i.e., M

has been changed from zero to N . When the M is less than 80, the NDOA obtains a high probability of recovery and shows superior recovery ratio than the traditional OMP and its improved algorithms, including ROMP, SWOMP and SP.

And then, we examined the relations between the reconstruction performance and the K -sparse.

Assuming the measurement number $M=64$, the performance of recovery were respectively observed in different algorithms of OMP, ROMP, SWOMP, SP and NDOA. The Fig.3 illustrates the probability of perfect reconstruction under 100 cycles with $N=96$, $M=64$, when the K -sparse has been changed from zero to N and the relative error of recovery, $e \leq 1E - 6$.

The Fig.3 shows that the ratio of accurate reconstruction in different algorithms under

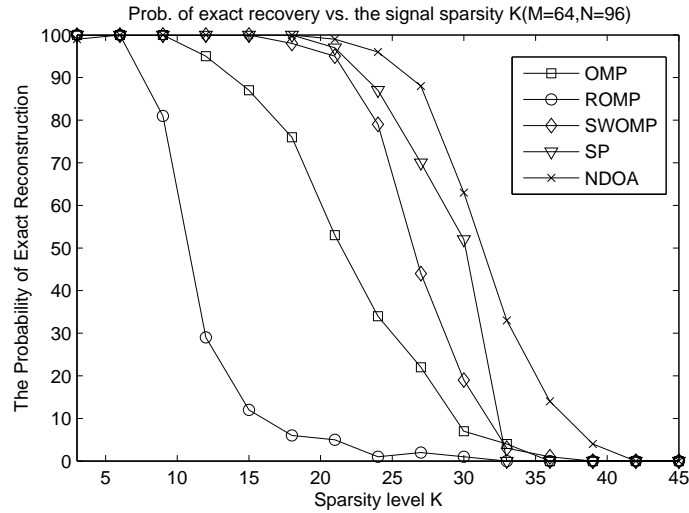


FIGURE 3. Perfect recovery probability versus the different K -sparse while $N=96$ and $M=64$

the random vector x with $N=96$, $M=64$, while only the K -sparse has been changed from zero to N . When the K is more than 15, the NDOA achieves higher probability of recovery than OMP, ROMP, SWOMP and SP algorithm.

3.3. Reconstruction performance for 2D image. In order to verify the effectiveness of the NDOA recovery for 2D image, we used 64×64 Lena image as an original and made it sparse by using the sym8 wavelet.

The peak signal to noise ratio (PSNR) and the relative error of recovery (R_{EOR}) had been separately defined as shown in (14) and (15), to evaluate the performance of accurate recovery.

$$PSNR = 10 \log_{10} [255^2 / (\frac{1}{m \times n} \|X - \hat{X}\|_2)] \quad (14)$$

$$R_{EOR} = \|X - \hat{X}\|_2 / \|X\|_2 \quad (15)$$

Now we proposed a parameter as $\eta = M/N$ to determine the sampling frequency for original image. When $\eta = 0.875$, we compared the effects of recovery with OMP, SWOMP and NDOA, respectively. The original Lena (64×64) and its discrete wavelet transform (DWT) image are shown in Fig.4. And the Fig.5 illustrates the recovery performance by using OMP algorithm, while the Fig.6 indicates the recovery by SWOMP and the Fig.7 demonstrates the recovery by NDOA.

To obtain an improved reconstruction achievement of the NDOA, Table 1 shows the

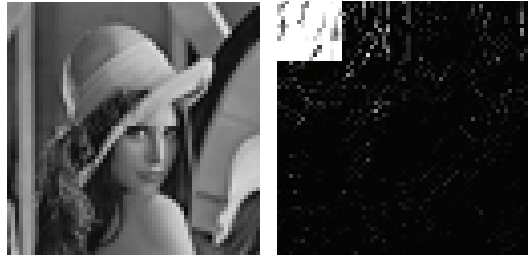


FIGURE 4. Lena and its DWT image

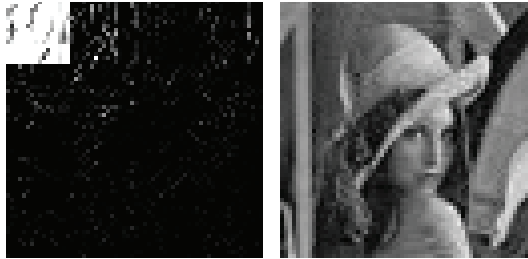


FIGURE 5. Recovery image by OMP

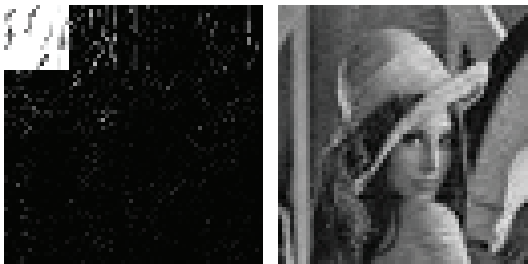


FIGURE 6. Recovery image by SWOMP

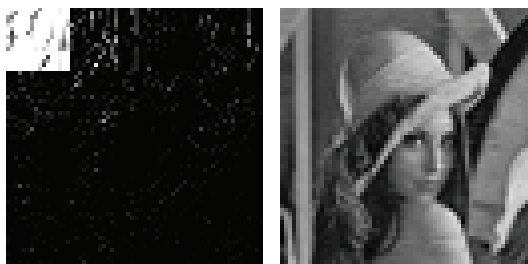


FIGURE 7. Recovery image by NDOA

value of PSNR and R_{EOR} of Lena image in different algorithms. From the statistical results in Table 1, every algorithm is done well in recovering the 2D image under the compressed sampling ratio $\eta = 0.875$. But the NDOA's PSNR is larger than the OMP and SWOMP with $3.6466dB$ while the R_{EOR} is decreased 2.21% at least. Therefore, the NDOA recovery preferment is more effective than OMP and SWOMP algorithm.

4. Conclusions. This paper proposed a CS reconstruction model based on NDOA with l_1 -norm optimization, and applied it to the 2D image recovery. Simulation experiment results show that the NDOA is more effective than the OMP, ROMP, SWOMP and

TABLE 1. Performance of different recovery algorithms

original image	recovery algorithm	sampling rate	PSNR /dB	$R_{EOR}/\%$
Lena image (64×64)	OMP	0.875	30.1562	7.23
	SWOMP	0.875	31.1756	6.43
	NDOA	0.875	34.8222	4.22

SP algorithms in performance of sparse signal recovery, and the probability of correct recovery is even higher under the condition of less observations and poor sparsity. When applying this model to 2D image recovery with compressed sampling rate of 0.875 for 64×64 Lena image, in comparison with the OMP and SWOMP, the NDOA's PSNR is raised by 3.6466dB while the R_{EOR} is decreased 2.21% at least. The reconstruction effect of NDOA is evidently excellent. This proposed algorithm can be used for wavelet filtering with CS or may as well be used as an efficient tool for digital signal compression or image painting. To find more proper composite filtering methods in the CS transform domain are our future works.

Acknowledgment. This work is partially supported by the National Natural Foundation Project (61304199), the Ministry of Science and Technology Project for Taiwan, Hongkong and Maco (2012DFM30040), the Major Projects in Fujian Province (2013HZ0002-1, 2013YZ0002, 2014YZ0001), the Science and Technology Project in Fujian Province Education Department (JB13140/GY-Z13088), the Scientific Fund Projects in Fujian University of Technology (GY-Z13005,GY-Z13125), and the 13th Five-Year planning project of Fujian Provincial Education Science (FJJKCGZ16-018).

REFERENCES

- [1] L. C. Jiao , S. Y. Yang , F. Liu , and B. Hou, Development and prospect of compressive sensing, *Tien Tzu Hsueh Pao/acta Electronica Sinica*, vol. 39, no.7, pp. 1651-1662, 2011.
- [2] M. F. Duarte , M. A. Davenport, D. Takbar , and J. N. Laska , Single-pixel imaging via compressive sampling, *IEEE Signal Processing Magazine*, vol. 25, no.2, pp. 83-91, 2008.
- [3] B. Han , F. Wu, D. Wu, Image representation by compressive sensing for visual sensor networks, *Journal of Visual Communication & Image Representation*, vol. 21, no.4, pp. 325-333, 2010.
- [4] G. Chen, D. Li, J. Zhang, Iterative gradient projection algorithm for two-dimensional compressive sensing sparse image reconstruction, *Signal Processing*, vol. 104, no. 6, pp. 15-26, 2014.
- [5] T. Cheng , G. B. Zhu, Y. A. Liu, Directional remote sensing and change detection based on two-dimensional compressive sensing. *Journal of Infrared and Millimeter Waves*, vol. 32, no. 5, pp.456-461, 2013.
- [6] Y. Zhou, F. Z. Zeng, An Image Retrieval Algorithm Based on Two-Dimensional Compressive Sensing and Hierarchical Feature, *Acta Electronica Sinica*, vol. 44, no. 02, pp. 453-460, 2016.
- [7] R. Zhou , *Several Kinds of Methods for Solving Bound Constrained Optimization Problems*, Ph.D. Thesis, Hunan University, Changsha, China, 2012.
- [8] E. J. Candès , J. Romberg, T. Tao, Robust uncertainty principles: exact signal reconstruction from highly incomplete frequency information, *IEEE Transactions on Information Theory*, vol. 52, no.2, pp. 489-509, 2006.
- [9] A. Malek, M. Alipour, Numerical solution for linear and quadratic programming problems using a recurrent neural network, *Applied Mathematics and Computation*, vol.192, no.1, pp.27C39, 2007.
- [10] Y. S. Xia, T. P. Chen, J. J. Shan, A novel iterative method for computing generalized inverse, *Neural Computation*, vol. 26, no. 2, pp. 449-465, 2014.
- [11] F. Xiong, Q. S. Yang, Neurodynamic optimization method for recovery of compressive sensed signals, *Application Research of Computers*, vol. 32, no. 8, pp. 2551- 2557, 2015.
- [12] H. C. Huang , F. C Chang ., Error resilience for compressed sensing with multiple-channel transmission, *Journal of Information Hiding and Multimedia Signal Processing*, vol. 6, no. 5, pp. 847-856, 2015.

- [13] M. Zhao , A. H. Wang , B.Zeng, L. Liu, H. H. Bai , Depth coding based on compressed sensing with optimized measurement and quantization, *Journal of Information Hiding and Multimedia Signal Processing*, vol. 5, no. 3, pp. 475-484, 2014.
- [14] DAI Qiong-Hai, FU Chang-Jun, JI Xiang-Yang, Research on Compressed Sensing, *Chinese Journal of computers*, vol. 34, no. 3, pp. 425-434, 2011.
- [15] X. Y. Sun , W. M. Song , Y Lvi , L. L.Tang , A new compressed sensing algorithm design based on wavelet frame and dictionary, *Journal of Information Hiding and Multimedia Signal Processing*, vol.5, no.2, pp. 234-241, 2014.
- [16] J. S. Pan ,W. Li, C. S. Yang, L. J. Yan , Image steganography based on subsampling and compressive sensing, *Multimedia Tools and Applications*, vol.74, no. 21, pp. 9191-9205, 2015.
- [17] T. Cheng , G. B. Zhu, X. L. Li, Equivalent Two-dimensional Sparse Transform of Compressive Sensing, *Semiconductor Optoelectronics*, vol. 35, no. 6, pp. 1119-1122, 2014.
- [18] L. I. Zhi-Lin , H. J. Chen , L. I. Ju-Peng , Yao C., and Yang, N., An Efficient Algorithm for Compressed Sensing Image Reconstruction, *Acta Electronica Sinica*, vol. 39, no. 12, pp. 2796-2800, 2011.
- [19] Y. S. Xia, A new neural network for solving linear and quadratic programming problems, *IEEE Transactions on Neural Networks*, vol. , no. 6, pp. 1544-1548, 1996.